PD-1 Protects Liver Damage by Suppressing IFN-γ Expression in T Cells in Infants and Neonatal Mice

Xuangjie Guo
Guangzhou Women and Children's Medical Center, Guangzhou Medical University
Yiping Xu
Guangzhou Women and Children's Medical Center, Guangzhou Medical University
Wei Luo
Guangzhou Women and Children's Medical Center, Guangzhou Medical University
Li Cai
Guangzhou University of Chinese Medicine
Ping Wang
Guangzhou Women and Children's Medical Center, Guangzhou Medical University
Yuxia Zhang
Guangzhou Women and Children's Medical Center, Guangzhou Medical University
Zhe Wen
Guangzhou Women and Children's Medical Center, Guangzhou Medical University
Yanhui Xu (yanhui.xu@zhanglaboratory.com)
Guangzhou Women and Children's Medical Center, Guangzhou Medical University

Research Article

Keywords: Biliary atresia, PD-1, IFN-g

Posted Date: April 16th, 2021

DOI: https://doi.org/10.21203/rs.3.rs-385311/v1

Version of Record: A version of this preprint was published at BMC Pediatrics on July 16th, 2021. See the published version at https://doi.org/10.1186/s12887-021-02794-x.

Abstract

Background: Biliary atresia (BA) is a severe cholangiopathy resulting from virus-induced and immune-mediated injury of the biliary system. IFN-g, secreted from $CD4^+$ Th1 cells and $CD8^+$ cytotoxic T cells, is a major mediator of liver pathology. Programmed death 1 (PD-1) signaling suppresses T cell function. However, how PD-1 modify T cell function in BA remains incompletely understood.

Methods: Frequencies of PD-1 expressing $CD4^+$ and $CD8^+$ T cells were analyzed in the liver and blood from BA and control subjects. Associations of $PD\text{-}1^+CD4^+/CD8^+$T cell abundances with liver function indices were measured. Function of PD-1 was measured by administration of an anti-PD-1 antibody in a Rhesus Rotavirus (RRV)-induced BA model. Survival, histology, direct bilirubin, liver immune cell subsets and cytokine production were analyzed.

Results: PD-1 was significantly upregulated in $CD4^+$ and $CD8^+$ T cells in patients with BA compared with control subjects. PD-1 expression in T cells was negatively associated with IFN-γ concentration in liver. Blockade of PD-1 increased IFN-g expression in $CD4^+$ T and $CD8^+$ T cells, suppressed bilirubin production and exacerbated liver immunopathology.

Conclusions: PD-1 plays a protective role in infants with BA by suppressing IFN-g production in T cells. Increasing PD-1 signaling may serve as a therapeutic strategy for BA.

Background

Biliary atresia (BA) is a disease of the biliary system presenting in infancy with poor prognosis and high mortality [1, 2]. If uncorrected, BA results in death within first two years of life. Although the symptoms could be partially improved by Kasai surgery, ~50% patients continue develop into liver failure and BA remains the major cause for childhood liver transplantation [3, 4]. A popular hypothesis of BA pathogenesis is that a primary perinatal cholangiovirus infection initiates an autoimmune response against the bile duct epithelium, while a secondary chronic inflammation mediates bile duct injury and fibrosis [5]. Studies using patients biopsies [6] and rotavirus-induced BA mouse models provide strong evidence for virus-induced autoimmune pathways [7, 8]. We [9] and others [7, 9, 10] have shown that IFN-g, secreted from $CD4^+$ T helper 1 (Th1) cells, ex-$CD4^+$ T helper 17 (Th17) T cells and $CD8^+$ T cells, are involved in the pathogenesis of BA. IFN-γ^+ cells are present within the portal tracts in the livers of infant with biliary atresia [11]. Blockade of IFN-γ is sufficient to prevent liver damage in rhesus rotavirus (RRV)-induced BA models in neonatal mice [12]. These findings support the notion that Th1 cell–mediated inflammation plays an important role in BA pathogenesis.

Programmed cell death 1 (PD-1) is a critical inhibitory molecule that suppresses IFN-g production by T cells and maintains peripheral tolerance [13]. When PD-1 or PD-L1 was deficient in NOD mice, onset and prevalence of type 1 diabetes (T1D) were accelerated, associating with an enhanced Th1 infiltration into the islets of pancreas [14]. In mouse model of autoimmune encephalomyelitis, blocking PD-1 or PD-L1/2

increased disease severity by promoting lymphocytes entry to the central nervous system [15]. Therefore, PD-1/PD-L1 appear to be involved in the development of autoimmune diseases in murine models. However, the role of PD-1 signaling in BA remains to be clarified.

Here, we examined PD-1 expression in patients with BA and in RRV-induced BA mice. We found that PD-1 was highly elevated in T cells in BA and its blockade augmented IFN-g production and liver pathology.

Materials And Methods

BA cohort

We recruited a cohort of children from the Department of Pediatric Surgery at Guangzhou Women and Children's Medical Center between January 2020 and January 2021. BA (n = 82) (median age: 2 months, ranging from 1 month to 7 months; male/female=0.43) was diagnosed according to intraoperative cholangiography when the intrahepatic biliary tree and/or extrahepatic bile duct could not be observed. All BA patients involved were full-term infants. For controls, children with normal liver function but requiring surgery for choledochal cyst (CC) (n = 16) (median age: 2 years 6 months, ranging from 3 month to 7 years old; male/female =0.45) were included.

Flow cytometry

Liver biopsies obtained from patients during laparoscopy or Kasai's operation were processed according to published procedures by Wang. et al [9]. Peripheral blood mononuclear cells or hepatic lymphocytes were incubated for 45 min at 4℃ with saturating concentrations of fluorescently labeled antibodies and analyzed on a FACSAria SORP flow cytometer (BD Science). Lymphocyte gating was performed based on the forward and side scatter pattern, followed by dead cell exclusion using propidium iodide (PI) in all surface staining samples.

RRV-induced mouse model of BA and anti-PD-1 treatment

All experimental wild-type BALB/c mice were SPF rated and placed in a room with a 12-hour dark/light cycle. Mice were injected intraperitoneally (i.p.) at 12-18 hours of birth with 30μl (1.5×10^{6} PFU/ml) rhesus rotavirus (RRV) or 0.9% saline (Control mice). RRV-infected mice that died within the first two days were excluded from the study. The clinical symptoms of BA development include yellowing of the skin and sclera, acholic stool, and growth retardation. RRV-infected mice were randomized into BA-RRV group or anti-PD-1 group. A total of four doses of anti-PD-1 antibody (50mg/kg) were given by i.p. injection every 3 days, starting on day 1 of life. Mice were sacrificed at 12 days after RRV, saline, RRV+anti-PD-1 treatment.

Liver function indices

Blood was collected by heart puncture and centrifuged at 13,000 r.p.m 4 ˚C for 5 min. Serum was collected for liver function measurement. ALT, AST, DB, TB were measured with liver function Assay (an automated clinical chemistry analyzer (Beckman Coulter AU5811, USA)).

Histopathology

The fresh liver tissues were fixed with 4% paraformaldehyde and embedded in paraffin, then sectioned (2 mm in thickness) and stained with hematoxylin and eosin (H&E) for morphological evaluation and Masson's trichrome staining for fibrosis.

Intracellular cytokine staining

Lymphocytes isolated from liver biopsies of patients or mice models were cultured on V-bottom 96-well plates in RPMI 1640 (Gibco) medium (R10) containing 10% heat-inactivated FBS (Gibco), 100 U/ml penicillin/streptomycin (Gibco) and 100 μM nonessential amino acids (Gibco) at 37℃ in 5% CO_2. 100 ng/ml Phorbol 12-myristate 13-acetate (PMA, Sigma-Aldrich, St Louis, MO), 2 μM/ml Ionomycin (Sigma-Aldrich) and 2 μM/ml monensin (Sigma-Aldrich) were used to stimulate the lymphocytes for 4-6 hours [9]. Intracellular staining was performed using eBioscience™ Intracellular Fixation & Permeabilization Buffer Set (Invitrogen) following the manufacturer's protocol. Briefly, stimulated cells were surface stained prior to fixation on ice for 20-30 minutes. Then cells were stained for intracellular cytokines at 4℃for 1 hour and resuspended in FACS buffer (PBS+2%FBS) before analysis by flow cytometry.

Statistical analysis

Prism 7.0 (GraphPad Software) was used for statistical analysis. Unpaired t test was used for two group analysis and one-way ANOVA for three or more group analysis. Non-parametric data were analyzed by Mann-Whitney U test or Kruskal-Wallis test. For all analyses, 2-tailed p values were calculated. P values for multiple comparisons were adjusted by the Benjamini- Hochberg method (Benjamini and Hochberg, 1995). All data points are shown with central lines indicating medians unless stated otherwise.

Results

PD-1 is highly expressed in T cells in the blood and liver of infants with BA

To reveal relevance of PD-1 expression and disease process of BA, we first examined PD-1 expression on $CD4^+$ T and $CD8^+$ T cells from peripheral blood mononuclear cells (PBMC) and liver biopsies.

Representative gating strategies were shown in Figure S1. We found that the percentages of PD-1 were significantly increased in hepatic $CD4^+$ T cells as well as blood and hepatic $CD8^+$ T cells in infants with BA compared with control subjects (Figure 1A-B).

PD-1 expression is negatively associated with IFN-g concentration in the liver of infants with BA

To demonstrate the function of PD-1, we measured its expression with liver IFN-g concentrations. We found that IFN-γ concentration in liver homogenates was negatively correlated with the frequencies of $PD\text{-}1^+CD4^+$ T and $CD8^+$ T cells (Figure 2A). Of liver function indices, we found that PD-1 expression was positively associated serum bilirubin concentrations (Figure 2B). Bilirubin is a heme breakdown product and has been shown as a potent anti-oxidant [16] and immune-suppressive agent of T cell activation [17]. Notably, percentages of PD-1 expression in T cells were not associated with other liver enzymatic indices (ALT, AST, GGT, AKP) or time of native liver survival (Figure S2A-E). Together, these data indicated that PD-1 expression may suppress IFN-g expression in T cells and reduce oxidative damage via bilirubin.

Blockade of PD-1 aggravates Liver pathology in RRV-induced model of biliary atresia

To validate these findings in vivo, we investigated an RRV-induced BA mouse model in neonatal BALB/c mice. We confirmed that PD-1 expression was significantly increased in $CD4^+$ and $CD8^+$ T cells in the liver of BA mice (Figure 3A). We then administered an anti-PD-1 blocking antibody in RRV-infected mice (Figure 3B), and found that liver damage was aggregated. Blocking PD-1 shifted jaundice to an earlier time (Figure 3C) and significantly decreased overall survival compared with untreated RRV mice (Figure 3D). Histologic analysis of livers also revealed more necrosis foci and lymphocytes accumulation around the portal tracks in liver of anti-PD-1 treated mice (Figure 3E). Furthermore, ALT and AST were significantly elevated (Figure 3F) in anti-PD-1 treated RRV mice. Similar to findings in BA patients, we observed significant down-regulation of total and direct bilirubin concentrations in anti-PD-1 treated RRV-mice (Figure 3G) . These data confirm that PD-1 expression play a protective role in limiting RRV-induced liver damage.

Blockade of PD-1 augments IFN-g expression in RRV-induced BA mice

To confirm that PD-1 protects liver damage via suppressing IFN-g expression in T cells, we next examined T cell function in RRV-induced BA model. We found that anti-PD-1 treatment promoted IFN-γ expression in both $CD4^+$ and $CD8^+$ T cells (Figure 4A-B). T-bet, the master transcription factor of Th1, was also highly elevated in the liver of anti-PD-1 treated RRV mice (Figure 4C). Consistently, plasma levels of IFN-γ and IL-

12P70 were elevated by PD-1 blockade (Figure 4D). Notably, anti-PD-1 treatment did not alter Foxp3$^+$ Treg cells in RRV-induced BA model (Figure 4E). Taken together, these data strengthen that PD-1 may have a protective role in alleviating BA liver damage by suppressing IFN-g expression in T cells.

Discussion

In the present study, we showed that PD-1 was highly elevated in CD4$^+$ and CD8$^+$ T cells in liver biopsies of infants with BA. High PD-1 expression was associated with low IFN-g but higher bilirubin concentrations. Using RRV-induced BA model, we demonstrated that PD-1 directly suppressed IFN-g but promoted bilirubin production.

PD-L1 is expressed on sinusoidal endothelial cells (LSEC), Kupffer cells, hepatocytes and stellate cells [18]. Interactions between PD-1$^+$CD4$^+$/CD8$^+$T cells and PD-L1 expressing cells in liver of BA play a protective role in limiting BA pathogenesis. IFN-γ production was negatively correlated with the frequencies of PD-1$^+$CD4$^+$ and CD8$^+$ T cells. PD-1 blockade in RRV induced BA mice contributed to an earlier onset of jaundice, enhanced Th1 response, and aggravated pathological injury of the liver. Unexpectedly, we found positive correlation between PD-1 expression and bilirubin concentration. When PD-1 was blocked, reduced bilirubin level was associated with abnormal increase of other liver function markers (ALT and AST). As a hormone, mildly elevated bilirubin levels have been newly established to be protective. Under inflammatory settings, bilirubin administration reduces TNF-a production by inhibiting iNOS but promoting prostaglandin E2 production [19].

Conclusion

In summary, we found increased frequencies of PD-1 expressing CD4$^+$ and CD8$^+$T cells in the livers of infant with BA. We propose PD-1 elevation may limit liver damage by simultaneously suppressing IFN-g production and oxidative damage. These findings may facilitate development of BA treatment strategies by harnessing the protective role of PD-1 signaling.

Abbreviations

BA:	Biliary atresia
PD-1:	Programmed death 1
RRV:	Rhesus-rotavirus
T1D:	Type 1 diabetes
SPF:	Specific Pathogen Free
AST:	Aspartate aminotransferase
GGT:	-glutamyl transpeptidase
AKP:	Alkaline phosphatase
ALT:	Alanine aminotransferase
PBMC:	Peripheral blood mononuclear cells

Declarations

Ethics approval and consent to participate

The Medical Ethics Committee of Guangzhou Women and Children's Medical Center approved the study procedures (ID:2019-21000). The implementations were in concordance with the International Ethical Guidelines for Research Involving Human Subjects as stated in the Helsinki Declaration. The legal guardians of all participants signed the informed contents. All animal experiments were approved by the Institutional Animal Care and Use Committee of Guangzhou Medical University, Guangzhou, China. The study was carried out in compliance with the ARRIVE guidelines (http://www.nc3rs.org.uk/page.asp?id=1357).

Consent for publication

Written parental consents for the publication have been obtained.

Availability of data and materials

The datasets used and/or analyzed during the current study are available from the corresponding author on reasonable request.

Competing interests

The authors have no financial and non-financial conflicts of interest.

Funding

This work was supported by the National Natural Science Foundation of China (92042303).

Author contributions statement

All authors have worked on the manuscript. YX (Yanhui Xu), XG and YX (Yiping Xu) performed laboratory experiments and wrote the article under the supervision of YZ. ZW performed Kasai procedure, treated and followed up the patient. YX (Yiping Xu), XG, ZW, PW, WL, LC participated in the process of samples collecting and follow ups.

Acknowledgement

This work was performed with funds from National Natural Science Foundation of China (92042303).

References

1. Asai, A., A. Miethke and J.A. Bezerra, Pathogenesis of biliary atresia: defining biology to understand clinical phenotypes. Nat Rev Gastroenterol Hepatol, 2015. 12(6): p. 342-52. https://doi.org/10.1038/nrgastro.2015.74.
2. Hartley, J.L., M. Davenport and D.A. Kelly, Biliary atresia. Lancet, 2009. 374(9702): p. 1704-13. https://doi.org/10.1016/S0140-6736(09)60946-6
3. Gallo, A. and C.O. Esquivel, Current options for management of biliary atresia. Pediatr Transplant, 2013. 17(2): p. 95-8. https://doi.org/10.1111/petr.12040
4. Bucuvalas, J.C., et al., Predictors of cost of liver transplantation in children: a single center study. J Pediatr, 2001. 139(1): p. 66-74. https://doi.org/10.1067/mpd.2001.115068
5. Petersen, C. and M. Davenport, Aetiology of biliary atresia: what is actually known? Orphanet J Rare Dis, 2013. 8: p. 128. https://doi.org/10.1186/1750-1172-8-128
6. Zheng, C., et al., Landscape of Infiltrating T Cells in Liver Cancer Revealed by Single-Cell Sequencing. Cell, 2017. 169(7): p. 1342-1356.e16. https://doi.org/10.1016/j.cell.2017.05.035
7. Mack, C.L., What Causes Biliary Atresia? Unique Aspects of the Neonatal Immune System Provide Clues to Disease Pathogenesis. Cell Mol Gastroenterol Hepatol, 2015. 1(3): p. 267-274. https://doi.org/10.1016/j.jcmgh.2015.04.001
8. Dong, R., et al., Forkhead box A3 attenuated the progression of fibrosis in a rat model of biliary atresia. Cell Death Dis, 2017. 8(3): p. e2719. https://doi.org/10.1038/cddis.2017.99
9. Wang, J., et al., Liver Immune Profiling Reveals Pathogenesis and Therapeutics for Biliary Atresia. Cell, 2020. 183(7): p. 1867-1883.e26. https://doi.org/10.1016/j.cell.2020.10.048

10. Yang, Y., et al., Elevated Th17 cells accompanied by decreased regulatory T cells and cytokine environment in infants with biliary atresia. Pediatr Surg Int, 2013. 29(12): p. 1249-60. https://doi.org/10.1007/s00383-013-3421-6
11. Mack, C.L., et al., Biliary atresia is associated with CD4+ Th1 cell-mediated portal tract inflammation. Pediatr Res, 2004. 56(1): p. 79-87. https://doi.org/10.1203/01.PDR.0000130480.51066.FB
12. Shivakumar, P., et al., Obstruction of extrahepatic bile ducts by lymphocytes is regulated by IFN-gamma in experimental biliary atresia. J Clin Invest, 2004. 114(3): p. 322-9.
13. Yokosuka, T., et al., Programmed cell death 1 forms negative costimulatory microclusters that directly inhibit T cell receptor signaling by recruiting phosphatase SHP2. J Exp Med, 2012. 209(6): p. 1201-17. https://doi.org/10.1084/jem.20112741
14. Wang, J., et al., Establishment of NOD-Pdcd1-/- mice as an efficient animal model of type I diabetes. Proc Natl Acad Sci U S A, 2005. 102(33): p. 11823-8. https://doi.org/10.1073/pnas.0505497102
15. Zamani, M.R., et al., PD-1/PD-L and autoimmunity: A growing relationship. Cell Immunol, 2016. 310: p. 27-41. https://doi.org/10.1016/j.cellimm.2016.09.009
16. Vasavda, C., et al., Bilirubin Links Heme Metabolism to Neuroprotection by Scavenging Superoxide. Cell Chem Biol, 2019. 26(10): p. 1450-1460.e7. https://doi.org/ 10.1016/j.chembiol.2019.07.006
17. Tran, D.T., et al., The Anti-Inflammatory Role of Bilirubin on "Two-Hit" Sepsis Animal Model. Int J Mol Sci, 2020. 21(22). https://doi.org/ 10.3390/ijms21228650
18. Oikawa, T., et al., Intrahepatic expression of the co-stimulatory molecules programmed death-1, and its ligands in autoimmune liver disease. Pathol Int, 2007. 57(8): p. 485-92.https://doi.org/10.1111/j.1440-1827.2007.02129.x
19. Wang, W.W., D.L. Smith and S.D. Zucker, Bilirubin inhibits iNOS expression and NO production in response to endotoxin in rats. Hepatology, 2004. 40(2): p. 424-33. https://doi.org/10.1002/hep.20334

Figures

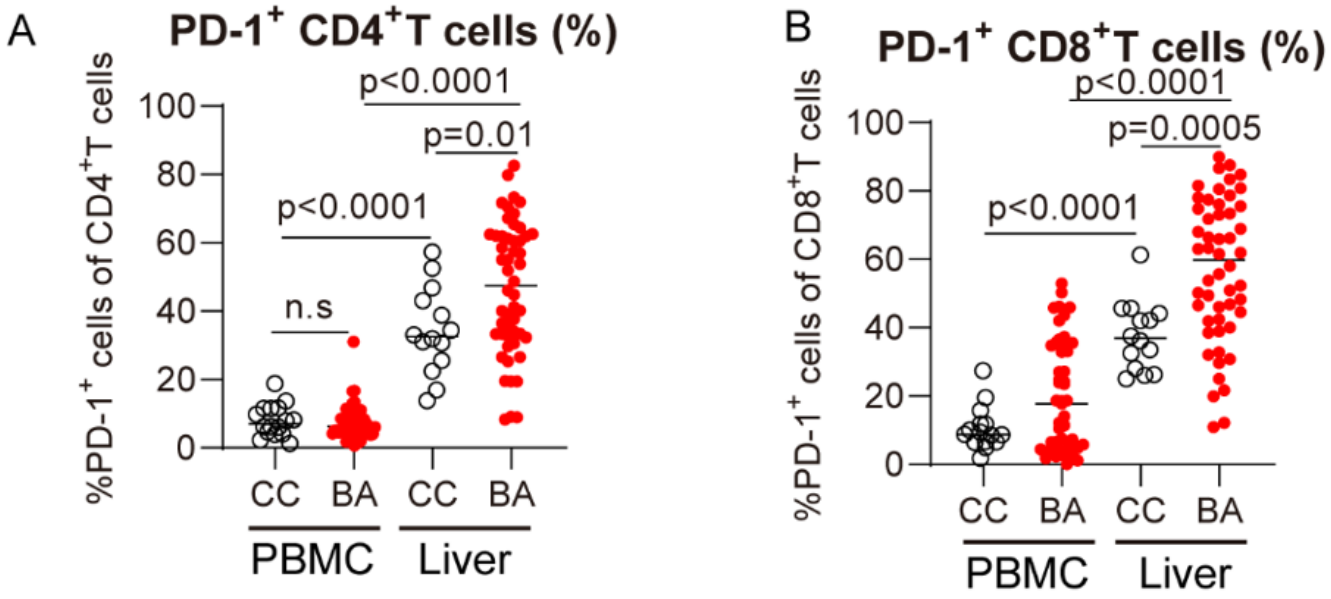

Figure 1

PD-1 expressing CD4+ and CD8+ T cells are increased in BA (A) Dot plots showing frequencies of PD-1+CD4+ T cells in BA and CC infants. Horizontal lines indicate median values. Significance was determined by Mann-Whitney U test. (B) Dot plots showing frequencies of PD-1+CD8+ T cells in BA and CC infants. Horizontal lines indicate median values. Significance was determined by Mann-Whitney U test.

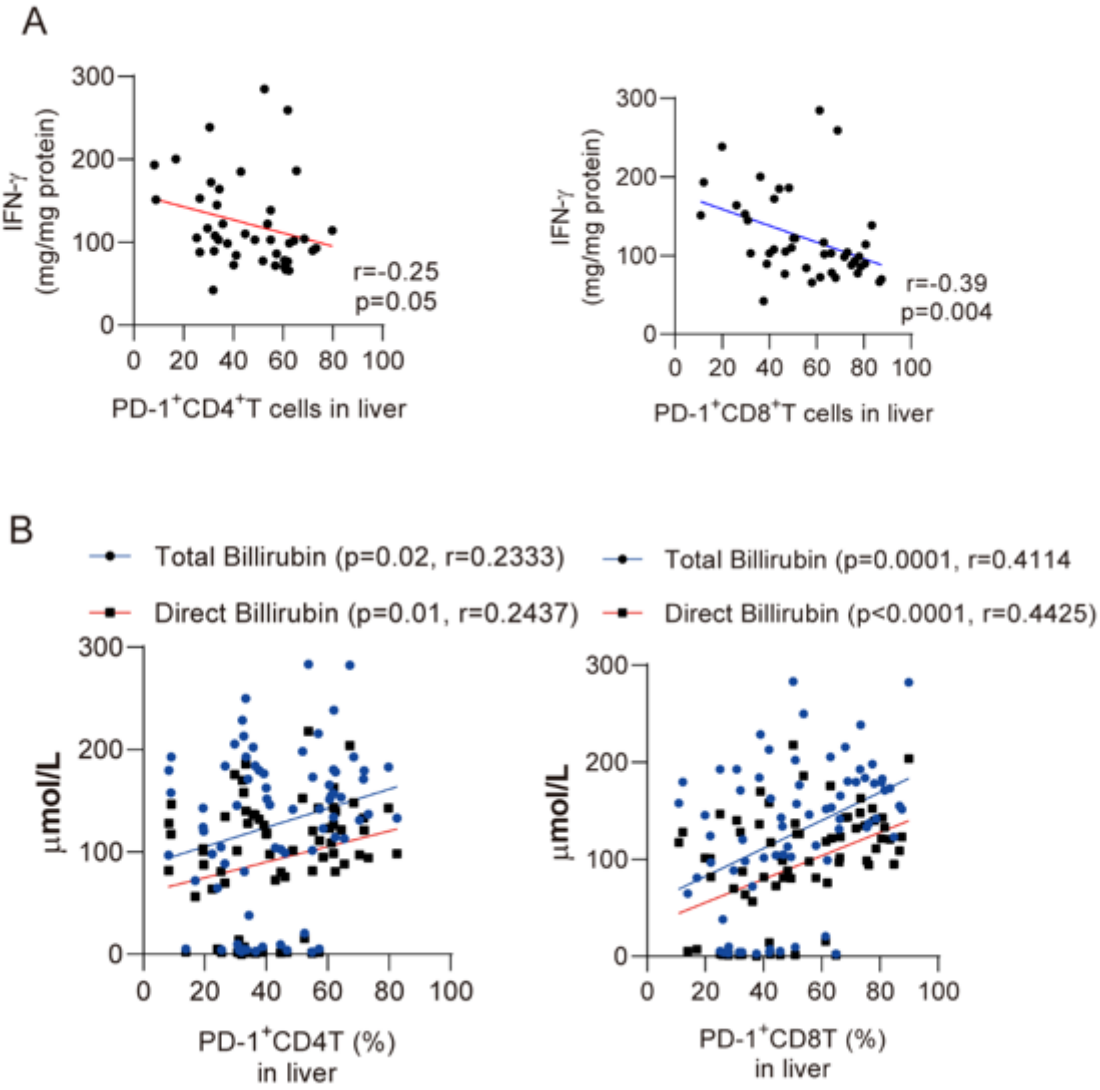

Figure 2

PD-1 expression is negatively associated with IFN-γ concentration in the livers of infants with BA (A) Scatter plots showing correlation between concentrations of IFN-γ with the frequencies of PD-1+CD4+T and PD-1+CD8+T cells in livers from BA and CC infants. (B) Scatter plots showing correlation between concentrations of total bilirubin and direct bilirubin with the frequencies of PD-1+CD4+T and PD-1+CD8+T cells in livers from BA and CC infants.

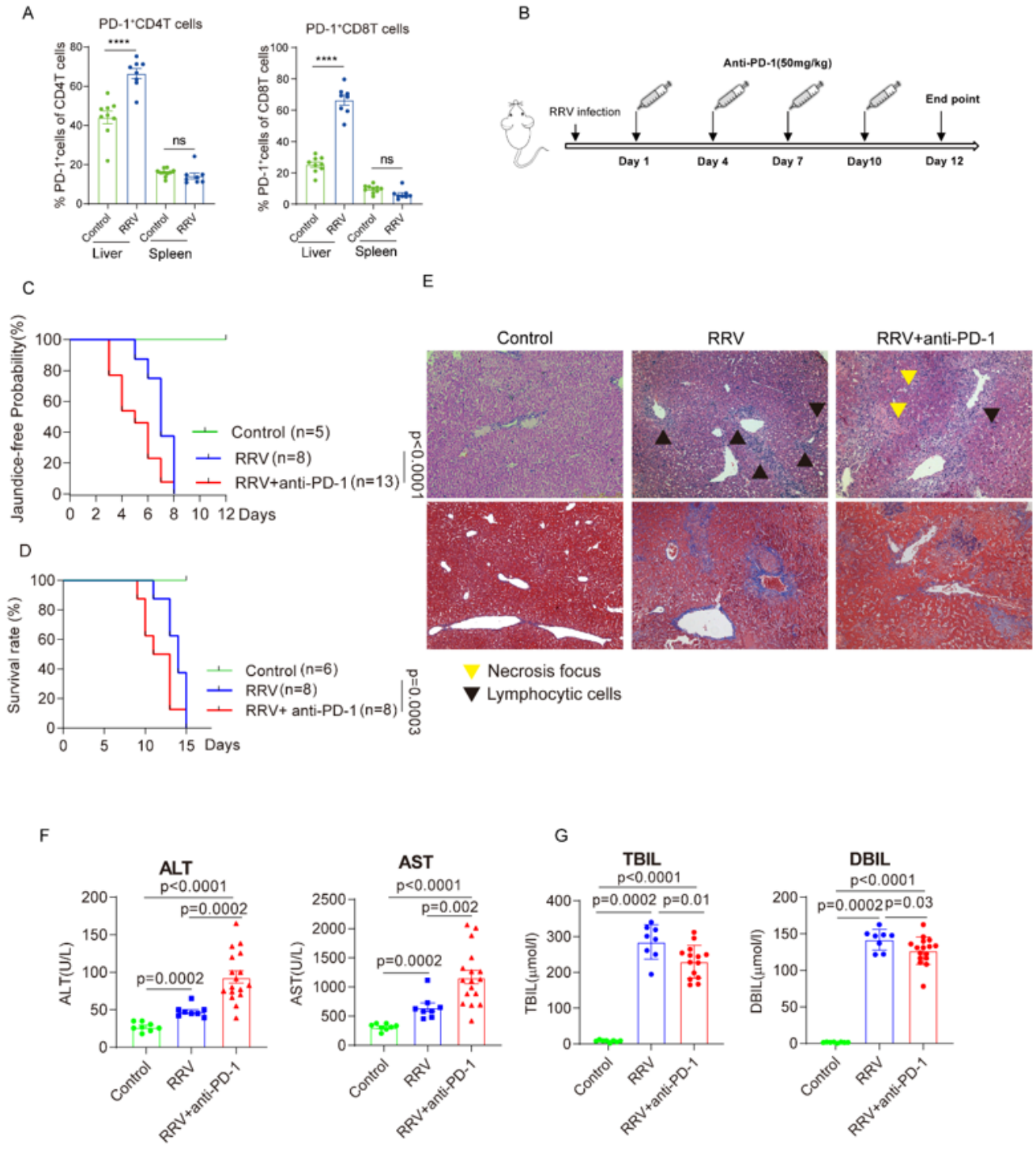

Figure 3

Blockade of PD-1 aggravates liver pathology in RRV-induced model of biliary atresia (A) Frequency of PD-1+ cells in CD4+ and CD8+T cells from livers and spleen of control（n=9) and BA mice (n=7). Data were expressed as mean ± SEM. Significance was determined by Student's t test;****p＜0.0001. (B) Schematic diagram of anti-PD-1 antibody administration. (C) Jaundice-free rates of control (n=5), BA mice (n=8), anti-PD-1 treated BA mice (n=13). Significance was determined by Log-rank test. (D) Survival rate of

control (n=5), BA mice (n=8), anti-PD-1 treated BA mice (n=13). Significance was determined by Log-rank test. (E) Hematoxylin and eosin (H&E, ×100) staining showing liver section from control, BA mice, anti-PD-1 treated BA mice. Yellow and black tangles indicate necrosis focus and lymphocytic cells, respectively. (F) Dot plots showing concentration of ALT and AST of control (n=5), BA mice (n=8), and anti-PD-1 treated BA mice (n=13). Data were expressed as mean ± SEM. Significance was determined by Student's t test. (G) Dot plots showing concentrations of total bilirubin (TBIL) and direct bilirubin (DBIL) of control (n=5), BA mice (n=8), and anti-PD-1 treated BA mice (n=13). Data were expressed as mean ± SEM. Significance was determined by Student's t test;

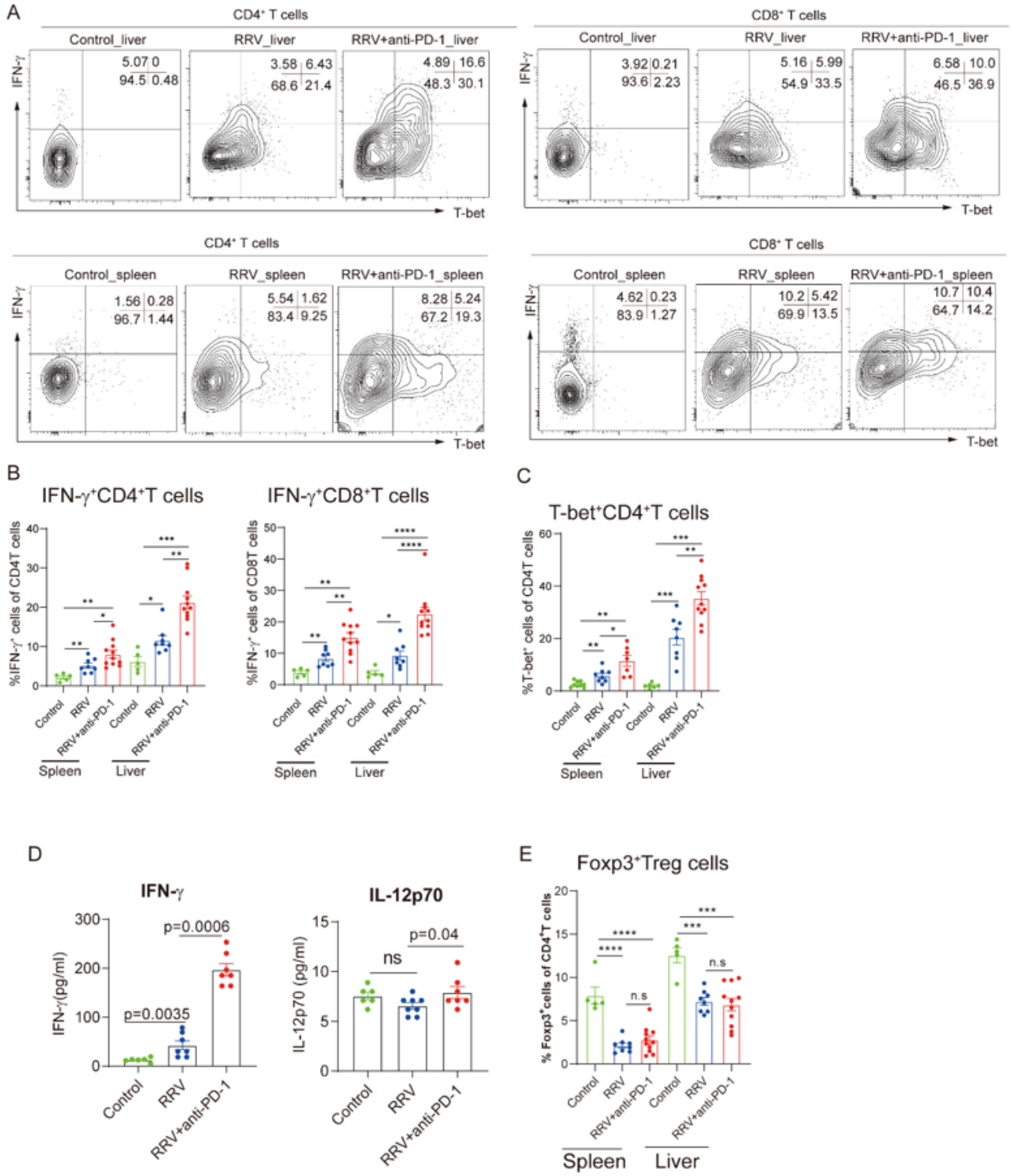

Figure 4

Blockade of PD-1 augments Th1 responses in RRV-induced BA mice (A) Flow cytometry gating strategies for intrahepatic IFN-γ expressing and T-bet expressing CD4+T and CD8+T cells in liver and spleen from control, BA mice, anti-PD-1 treated BA mice. (B) Dot plots showing percentages of IFN-γ+CD8+T and IFN-γ+CD4+T cells in liver and spleen from control (n=5), BA mice (n=8), and anti-PD-1 treated BA mice (n=13). Data were expressed as mean ± SEM. Significance was determined by Mann-Whitney U test,****p

0.0001,***p0.001,**p0.01. (C) Dot plots showing percentages of T-bet+CD4+ T cells in liver and spleen from control (n=5), BA (n=8), and anti-PD-1 treated BA mice (n=13). Data were expressed as mean ± SEM. Significance was determined by Mann-Whitney U test,****p0.0001,***p0.001,**p0.01. (D) Dot plots showing plasma levels of IFN- and IL-12p70 in control (n=5), BA mice (n=8),and anti-PD-1 treated BA mice (n=7). Data were expressed as mean ± SEM. Significance was determined by Mann-Whitney U test. (E) Dot plots showing percentage of Foxp3+Treg cells in liver and spleen from control (n=5), BA mice (n=8),and anti-PD-1 treated BA mice (n=13). Data were expressed as mean ± SEM. Significance was determined by Mann-Whitney U test,****p0.0001,***p0.001,**p0.01.

Supplementary Files

This is a list of supplementary files associated with this preprint. Click to download.

- FigureS1.docx
- FigureS2.docx